

LETTERS

No climate paradox under the faint early Sun

Minik T. Rosing^{1,2,4}, Dennis K. Bird^{1,4}, Norman H. Sleep⁵ & Christian J. Bjerrum^{1,3}

Environmental niches in which life first emerged and later evolved on the Earth have undergone dramatic changes in response to evolving tectonic/geochemical cycles and to biologic interventions^{1–3}, as well as increases in the Sun's luminosity of about 25 to 30 per cent over the Earth's history⁴. It has been inferred that the greenhouse effect of atmospheric CO₂ and/or CH₄ compensated for the lower solar luminosity and dictated an Archaean climate in which liquid water was stable in the hydrosphere^{5–8}. Here we demonstrate, however, that the mineralogy of Archaean sediments, particularly the ubiquitous presence of mixed-valence Fe(II–III) oxides (magnetite) in banded iron formations⁹ is inconsistent with such high concentrations of greenhouse gases and the metabolic constraints of extant methanogens. Prompted by this, and the absence of geologic evidence for very high greenhouse-gas concentrations^{10–13}, we hypothesize that a lower albedo on the Earth, owing to considerably less continental area and to the lack of biologically induced cloud condensation nuclei¹⁴, made an important contribution to moderating surface temperature in the Archaean eon. Our model calculations suggest that the lower albedo of the early Earth provided environmental conditions above the freezing point of water, thus alleviating the need for extreme greenhouse-gas concentrations to satisfy the faint early Sun paradox.

The Earth's surface environment over the approximately 4 billion years (Gyr) recorded in geologic formations appears to have been maintained within a relatively narrow range in which liquid water was stable. This is surprising because the factors that determine surface temperature have evolved owing to temporal variations of the Sun's irradiance, the Earth's albedo and cloud cover, and concentrations of atmospheric greenhouse gases over geologic time. It is not readily apparent to what extent this apparent thermostasis can be attributed to physico-chemical feedback mechanisms, metabolic interventions from living organisms, or combinations of unrelated secular changes.

A 25–30% lower solar luminosity from the early Sun inferred from standard stellar evolution trends⁴ should have caused a 21–26 K lower radiative equilibrium temperature for the early Earth, with a planetary albedo equal to the present value^{5,7}. If we also assume that the atmosphere had a transmittance similar to the present, then the average early Archaean surface temperature would have been below the freezing point of water. The contrast between geologic evidence for the presence of liquid water on the Earth's surface in the deep past^{15,16} with the lower irradiance from a faint early Sun has been cast as a paradox, prompting hypotheses^{5–8,17} of stronger greenhouse effects from high partial pressures of CO₂, NH₄, CH₄, and/or C₂H₆. Secular changes in the contribution from clouds to the Earth's planetary albedo have also been proposed as important parameters controlling climate on the early Earth^{18,19}.

Extreme concentrations of greenhouse gases would be required to support marine temperatures of 70 ± 15 °C, as suggested from oxygen isotopes of cherts 3.5–3.2 Gyr old and the assumption that the oxygen

isotope composition of Archaean sea water was the same as at present^{20,21}. Such high temperatures and required greenhouse gas concentrations, as well as the consistency of the oxygen isotope composition of sea water over geologic time, are not universally accepted^{22,23}, and would have required a partial pressure of atmospheric CO₂ of $p_{\text{CO}_2} \approx 2\text{--}6$ bar at ~3.3 Gyr ago (assuming $p_{\text{CH}_4} < 0.01$ bar). Furthermore, predicted changes in the oxygen isotope composition of sea water over geologic time is consistent with a warm, but not a hot, early Earth^{23,24}.

Geologic evidence provided from palaeosols 2.75–2.2 Gyr old^{13,25}, 3.2-Gyr-old weathering rinds of fluvial clasts¹², 3.5-Gyr-old and 3.2-Gyr-old evaporites³, and cycling of CO₂ in and out of the mantle taking into account the consequences of seafloor weathering¹¹: all predict atmospheric CO₂ concentrations insufficient to compensate for the faint early Sun. Extremes in limits of atmospheric CO₂ have been estimated on the basis of the presence or absence of siderite or an Fe(II)-rich layer-silicate in near-surface weathering environments, as well as mass-balance constraints of weathering recorded in Precambrian palaeosols. These estimates are illustrated in Fig. 1, where they can be compared to the stability fields of minerals in the system FeO–Fe₂O₃–SiO₂–CO₂–H₂O and also to several predicted limits of atmospheric p_{CO_2} required to satisfy the faint early Sun paradox.

Atmospheric concentrations of greenhouse gases can also be constrained by the mineralogy of shallow marine precipitates, specifically magnetite in Archaean banded iron formations⁹. We assume that the oceans and atmosphere were linked by gas exchanges across their interface. We do not imply that the atmosphere was in equilibrium with the rock substrate, but we do suggest that minerals abundantly precipitated in the shallow ocean (for example, the magnetite + siderite of banded iron formations) were not far from equilibrium with atmospheric gases. Magnetite (FeOFe₂O₃) is used as a proxy for the primary precipitate, although meta-stable mixed-valence Fe(II, III) hydroxides (fougerite, 'green rust') or Fe(II, III) hydroxycarbonates may have been present before conversion to more stable phases. Ohmoto *et al.*²⁶ proposed that atmospheric concentrations of CO₂ > 100 times PAL (the present atmospheric level of about 10^{–3.5} bar) were required to form siderite in the presence of Fe(III) hydroxides (goethite) in banded iron formations before ~1.8 Gyr ago. Phase relations shown in Fig. 1 demonstrate that such high concentrations preclude the stability of magnetite; furthermore, the stability of the assemblage siderite + goethite (represented in Fig. 1 by haematite) requires p_{H_2} to be several orders of magnitude below the lower limit for methanogenesis ($p_{\text{H}_2} > 10^{-5}$ bar), as illustrated by the yellow highlighted region in Fig. 1.

Conceptually, redox conditions are reflected by speciation of iron in marine precipitates and rocks produced through weathering and alteration of continental and oceanic crust. If the ocean and atmosphere were generally reducing, Fe(II) minerals would be favoured

¹Nordic Center for Earth Evolution, Øster Voldgade 5-7, ²Natural History Museum of Denmark, University of Copenhagen, Øster Voldgade 5-7, ³Department of Geography and Geology, University of Copenhagen, Øster Voldgade 10, DK-1350 København K., Denmark. ⁴Department of Geological and Environmental Sciences, ⁵Department of Geophysics, Stanford University, Stanford, California 94305, USA.

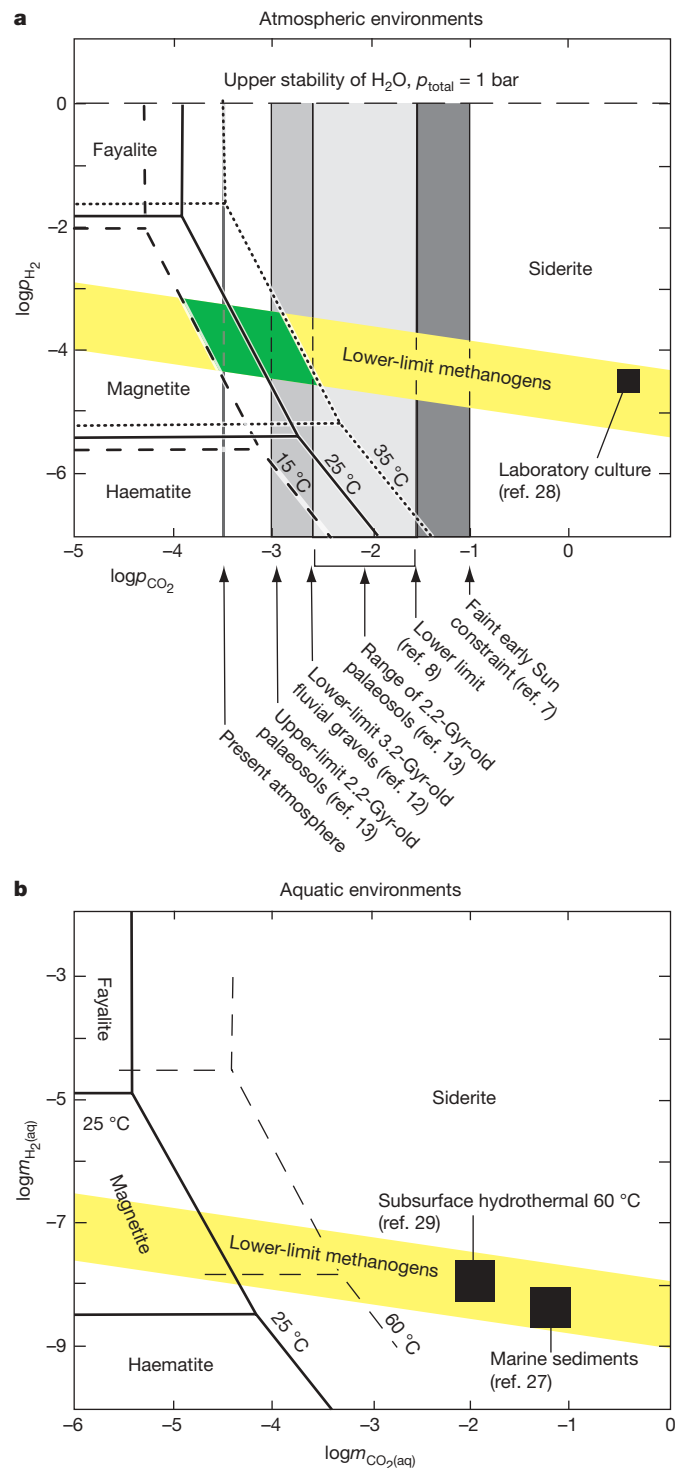
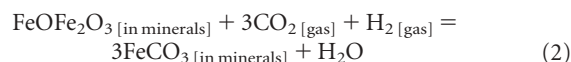


Figure 1 | Constraints on the partial pressures for CO₂ and H₂ in the atmosphere of the early Earth. Stability of minerals in the system FeO–Fe₂O₃–SiO₂–CO₂–H₂O at 1 bar total pressure for the given temperatures. **a, b**, Partial pressures (bar) (**a**) and aqueous concentrations (molalities) (**b**) of H₂ and CO₂. Solid squares indicate observed conditions for extant methanogens. The yellow band indicates the lower limit of H₂ for methanogenesis with a slope constrained by the stoichiometry of reaction (4) (see text). Model estimates for p_{CO_2} are indicated by arrows and vertical bars in **a**. The green shading denotes the stability range of magnetite + siderite between 15 °C and 35 °C at a p_{H_2} controlled by methanogens.

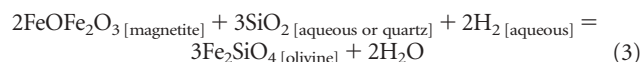
and Fe(III) compounds would break down owing to reduction of Fe(III). This oxidizes the environment by consuming H₂ through reactions of the type:



Likewise, increasing CO₂ would favour formation of siderite (FeCO₃) relative to Fe(II) silicates, and Fe(III)-containing minerals such as magnetite (FeOFe₂O₃) would react to form siderite while consuming hydrogen:



Ferric iron is present in the Earth's mantle and in mantle-derived melts where equilibria involving ferrous iron silicates and Fe(III)-rich spinels (nominally magnetite) define the intrinsic oxidation state of the Earth's mantle and crust. Ferrous iron silicates can be oxidized by water to form magnetite while releasing aqueous silica and hydrogen, which may escape to the ocean–atmosphere system through hydrothermal vents (the reverse of reaction (1)). Reactions involving fluids that have equilibrated with silica-rich rocks and/or CO₂-rich reservoirs such as the ocean–atmosphere system will, on the contrary, consume hydrogen as magnetite reacts to form Fe(II) carbonate through reaction (2) and to form Fe(II) silicates as illustrated by reaction (3), taking into account the fayalite component in olivine.



The mantle and its magmatic derivatives will thus be reducing relative to silica- and/or CO₂-poor fluids, but oxidizing relative to silica- and/or CO₂-rich fluids. The reverse of reaction (3) represents hydrothermal oxidation of ultramafic rocks producing magnetite and releasing H₂, which, together with CO₂, provides important niches for methanogenic bacteria^{1,2} according to:



Although the Gibbs energy of reaction (4) is dependent on temperature and the relative partial pressures (concentrations) of CO₂, H₂ and CH₄, extant methanogenic organisms that metabolize H₂ in subsurface and shallow marine environments are able to deplete H₂ to $\sim 10^{-5}$ bar (Fig. 1) where the Gibbs energy of reaction is about 9–15 kJ mol⁻¹ (refs 27–29). This would be in the range of about –3.5 to –4.5 at p_{CO_2} compatible with magnetite–siderite stability. This is the order of magnitude for the lower limit of predicted atmospheric H₂ on the early Earth determined by coupled atmospheric–ecosystem models involving metabolic processes of methanogens, acetogens and anoxygenic phototrophs^{30,31}. Conversion of H₂ to CH₄ or organic matter by hydrogen-consuming methanogens and phototrophs is in effect an oxidation of the environment, and like oxygen-producing phototrophs they build redox gradients in their environments, with higher oxidation levels in the photic zone and lower at deeper levels in the ocean. Such redox contrasts in the early Archaean ocean have been documented³² and perhaps the presence of H₂-metabolizing phototrophs might have controlled the atmospheric p_{H_2} at values close to 10^{-5} bar (Fig. 1).

We conclude from the phase relations in Fig. 1, and the prevalence of magnetite in Archaean chemical sediments, that CO₂ and H₂ mixing ratios in the early Earth's atmosphere were not significantly different from present-day values. If p_{H_2} is limited by the metabolic processes of methanogens ($\sim 10^{-5}$ bar) then CO₂ values of the order of about 3 times PAL are consistent with magnetite–siderite phase relations at about 25 °C (green shading in Fig. 1). Given the uncertainty in paragenetic relations, it appears that the geologic/thermodynamic constraints imposed by the mineralogy of soils¹³ and weathering products of fluvial sediments¹² are in accord with the mineralogy of shallow marine chemical sediments. Consequently,

the greenhouse effect of Archaean CO_2 levels was too small to compensate for the faint early Sun.

Methane has been suggested as an important greenhouse gas^{5,6,8}. Haqq-Misra *et al.*⁸ suggests an upper limit of $\text{CH}_4:\text{CO}_2 < 1-0.6$ in the atmosphere if the positive greenhouse effect should not be counterbalanced by a negative albedo effect from organic haze, and predict even lower mixing ratios of $\text{CH}_4:\text{CO}_2$. This requires CO_2 concentrations in excess of 100 PAL to account for the faint early Sun, which precludes the stability of mixed-valence Fe(II–III) oxides and requires other factors that could influence the radiation balance of the Earth and counteract the faint early Sun (Fig. 1). Methane and CO_2 concentrations allowed by the mineralogic and metabolic constraints of CO_2 and H_2 outlined in Fig. 1 are unable to provide sufficient greenhouse warming to offset the effect of the faint early Sun.

We now investigate the role of the Earth's planetary albedo, which is a major factor determining the Earth's surface temperature. Albedo is determined by the nature of the materials on the Earth's surface, and the abundance and type of clouds¹⁸. The difference in planetary albedo over land and oceans is minor today, partly because most land is covered by vegetation and partly because the top-of-the-atmosphere albedo is dominated by the contribution from clouds. Because the concentrations and type of cloud condensation nuclei (CCN) have evolved over geologic time, clouds over the early Earth had different characteristics. The droplet size in clouds is determined by the availability of CCN and the H_2O contents in the atmosphere. Few CCN results in larger droplets, less scattering of incoming short-wave radiation and a shorter lifetime of clouds. In our present atmosphere the majority of CCN are produced by atmospheric oxidation of gases released by plants and eukaryotic algae. With a non-oxygenic atmosphere and a biosphere devoid of plants and algae, CCN concentrations would probably have been considerably lower on the early Earth than they are today. This biotic effect on cloud formation through CCN can be observed over low-productivity gyres in the ocean today, where the transparency of the atmosphere for incoming short wave radiation is greater than in areas with high biologic productivity¹⁴. With a more transparent atmosphere the low albedo of the ocean would be more strongly expressed in the planetary albedo, as illustrated in Fig. 2 (see Methods).

We have modelled the sensitivity of the Precambrian radiation balance to changes in the fraction of the Earth's surface covered by continents as well as biological evolution over geologic time. The Earth's continents are formed by fractionation of the mantle through a suite of geological processes taking place over some span of time. There is little consensus on when the first continents emerged, or the rate of growth since continental nucleation. However, mass-balance considerations for radioactive tracers and their daughter isotopes in the mantle and crust have allowed construction of continental growth models, most of which support a sigmoidal increase in the mass of the continents, beginning at about 4 Gyr ago with a rapid growth rate between 3.5 and 1.5 Gyr ago and levelling out from about 1 Gyr ago to the present, as illustrated in Fig. 2a. There is no simple relationship between the mass of continental material extracted from the mantle and the surface area of exposed land, because a number of geophysical parameters, including the rheology of the Earth's mantle, influence the area/volume ratio for the continents. We have chosen to use the present-day area/volume relationship (Fig. 2a), which probably overestimates the continental area, and in consequence, the albedo for the early Earth. Because the timing and rate of growth of the Earth's continents is a matter of debate, we have included a scenario in which the surface area occupied by continents is constant over geologic time as one end-member in our model (see Methods).

Our model, which is based on that of Caballero and Steder³³, takes into account the effects of lower production of biogenic CCN, and lower average surface albedo (Fig. 2b) owing to less continental area to predict the temporal evolution of planetary albedo through geologic time (Fig. 2c) (see Methods). The results are summarized in Fig. 2d, where CO_2 and CH_4 are both 900 parts per million by volume

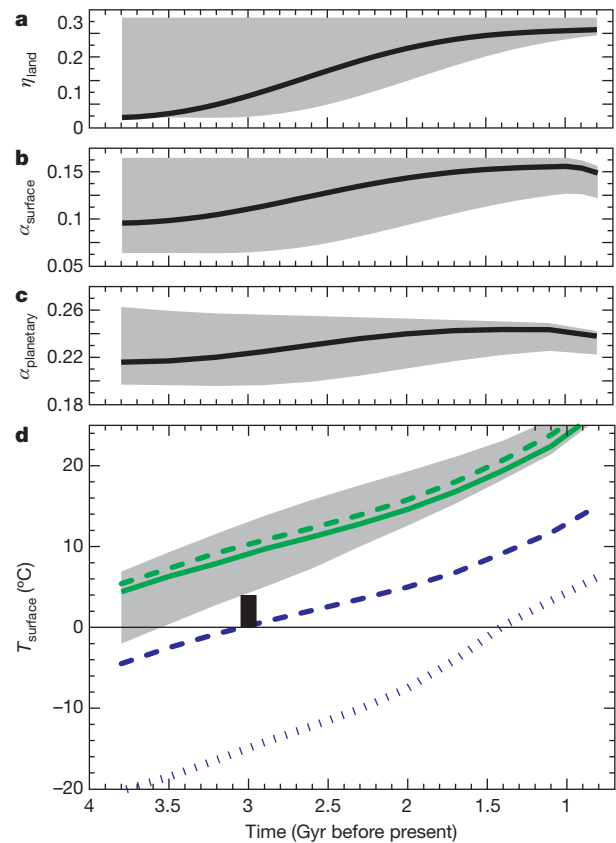


Figure 2 | Climatic models for the Earth since 3.8 Gyr ago. **a**, The continent fraction (η_{land}) of the Earth's surface as a function of geologic time. The solid line is based on geochemical models (see Methods). The shaded area includes uncertainties in the estimate of continental emergence and growth as well as the possibility that the continent area has remained constant. **b**, Surface albedo (α_{surface}) as a function of geological time (see Methods). The land albedo (α_{land}) is assumed to be granitic desert of albedo 0.3 gradually changing to the present vegetated land of albedo 0.21 from 1.0 Gyr ago (the contribution from ice albedo is assumed to be constant at the present level). The solid line is based on the growth model in **a**, and the shaded area is the range covered by the shaded area in **a**, assuming ice albedo proportional to η_{land} for the lower bound. **c**, The Earth's calculated average planetary albedo ($\alpha_{\text{planetary}}$) as a function of geological time for a droplet size of 30 μm and 900 p.p.m.v. CO_2 and 900 p.p.m.v. CH_4 . **d**, Surface temperature (T_{surface}) versus geologic time assuming increasing solar irradiance, α_{surface} scaled to the extent of continents from **b** and different average cloud droplet sizes. The blue lines are computed for 375 p.p.m.v. CO_2 and 1.7 p.p.m.v. CH_4 and droplet sizes of 20 μm (dashed line) and 12 μm (present-day size and water content; dotted line). The green lines are computed for droplet sizes of 20 μm (solid line) and 30 μm (dashed line) and 900 p.p.m.v. CO_2 and 900 p.p.m.v. CH_4 . The grey shading is the α_{surface} range in **b**. The black bar represents the model from ref. 18 with dynamically adjusted clouds but present optical properties of clouds.

(p.p.m.v.). This represents an intermediate p_{CO_2} level within the range of environmental conditions represented by the green shading in Fig. 1a. The model provides similar results as long as CO_2 is substituted for CH_4 in such a way that an increase of 7 p.p.m.v. units of CO_2 is balanced by a decrease of 1 p.p.m.v. unit of CH_4 . At the high- CO_2 extreme of the range in Fig. 1a, this corresponds to 800 p.p.m.v. for CH_4 and 1,600 p.p.m.v. for CO_2 .

Our model (Fig. 2) shows that the albedo effects of the growth of the Earth's continents, amplified by higher transparency for short-wave radiation of the early atmosphere, was sufficient to counterbalance the secular changes in irradiance from the Sun⁴ through geologic history. We suggest that the evidence for the presence of liquid water under the faint early Sun is not paradoxical⁵. The early Earth was dominated by oceans and lacked plants and algae, which resulted in a lower planetary albedo. Absorption of a higher fraction

of the incoming solar radiation in combination with only slightly higher concentrations of greenhouse gases, probably CO₂ and methane, provided the Earth with a clement climate.

METHODS SUMMARY

Mineral assemblages in chemical sediments preserved in the geologic record reflect the fugacities of dissolved gases in the Precambrian shallow ocean through reactions (1) to (3). Equilibrium fugacities of H₂ and CO₂ were calculated using the SUPCRT computer program, which calculates equilibrium constants for given temperatures and pressures using an internally consistent thermodynamic database for minerals, aqueous species and gases. In this study we used the SLOP98 database (see Methods). The effects of the changes in solar luminosity, in radiative transparency of the atmosphere by reduced CCN from plants and algae and the changes in surface albedo caused by continental growth and emergence of land vegetation were calculated by a radiative–convective equilibrium model based on the CliMT climate modelling toolkit³³ using the NCAR CCM3 radiation code. Details, references and links to the computer program sources are given in the Methods section.

Full Methods and any associated references are available in the online version of the paper at www.nature.com/nature.

Received 13 July 2009; accepted 9 February 2010.

- Canfield, D. E., Rosing, M. T. & Bjerrum, C. Early anaerobic metabolisms. *Phil. Trans. R. Soc. B* **361**, 1819–1834 (2006).
- Sleep, N. H. & Bird, D. K. Niches of the pre-photosynthetic biosphere and geologic preservation of Earth's earliest ecology. *Geobiology* **5**, 101–117 (2007).
- Lowe, D. R. & Tice, M. M. Geologic evidence for Archean atmospheric and climatic evolution: fluctuating CO₂, CH₄, and O₂, with an overriding tectonic control. *Geology* **32**, 493–496 (2004).
- Gough, D. O. Solar interior structure and luminosity variations. *Sol. Phys.* **74**, 21–34 (1981).
- Sagan, C. & Mullen, G. Earth and Mars—evolution of atmospheres and surface temperatures. *Science* **177**, 52–56 (1972).
- Kiehl, J. T. & Dickinson, R. E. A study of the radiative effects of enhanced atmospheric CO₂ and CH₄ on early Earth surface temperatures. *J. Geophys. Res.* **92**, 2991–2998 (1987).
- Kasting, J. F. Earth's early atmosphere. *Science* **259**, 920–926 (1993).
- Haqq-Misra, J. D., Domagal-Goldman, S. D., Kasting, P. J. & Kasting, J. F. A. Revised, hazy methane greenhouse for the Archean Earth. *Astrobiology* **8**, 1127–1137 (2008).
- Klein, C. & Beukes, N. in *Proterozoic Crustal Evolution* Vol. 10 *Developments in Precambrian Geology* (ed. Condie, K. C.) 383–418 (Elsevier, 1992).
- Rye, R., Kuo, P. H. & Holland, H. D. Atmospheric carbon-dioxide concentrations before 2.2-billion years ago. *Nature* **378**, 603–605 (1995).
- Sleep, N. H. & Zahnle, K. Carbon dioxide cycling and implications for climate on ancient Earth. *J. Geophys. Res. Planets* **106**, 1373–1399 (2001).
- Hessler, A. M., Lowe, D. R., Jones, R. L. & Bird, D. K. A lower limit for atmospheric carbon dioxide levels 3.2 billion years ago. *Nature* **428**, 736–738 (2004).
- Sheldon, N. D. Precambrian paleosols and atmospheric CO₂ levels. *Precamb. Res.* **147**, 148–155 (2006).
- Kump, L. R. & Pollard, D. Amplification of cretaceous warmth by biological cloud feedbacks. *Science* **320**, 195 (2008).
- Rosing, M. T., Rose, N. M., Bridgwater, D. & Thomsen, H. S. Earliest part of Earth's stratigraphic record: a reappraisal of the >3.7 Ga Isua (Greenland) supracrustal sequence. *Geology* **24**, 43–46 (1996).
- Peck, W. H., Valley, J. W., Wilde, S. A. & Graham, C. M. Oxygen isotope ratios and rare earth elements in 3.3 to 4.4 Ga zircons: ion microprobe evidence for high delta O-18 continental crust and oceans in the Early Archean. *Geochim. Cosmochim. Acta* **65**, 4215–4229 (2001).
- Catling, D. C., Zahnle, K. J. & McKay, C. P. Biogenic methane, hydrogen escape, and the irreversible oxidation of early Earth. *Science* **293**, 839–843 (2001).
- Rosow, W. B., Henderson-sellers, A. & Weinreich, S. K. Cloud feedback—a stabilizing effect for the early Earth. *Science* **217**, 1245–1247 (1982).
- Charlson, R. J., Lovelock, J. E., Andreae, M. O. & Warren, S. G. Oceanic phytoplankton, atmospheric sulfur, cloud albedo and climate. *Nature* **326**, 655–661 (1987).
- Knauth, L. P. & Lowe, D. R. High Archean climatic temperature inferred from oxygen isotope geochemistry of cherts in the 3.5 Ga Swaziland Supergroup, South Africa. *Geol. Soc. Am. Bull.* **115**, 566–580 (2003).
- Tice, M. M. & Lowe, D. R. Photosynthetic microbial mats in the 3,416-Myr-old ocean. *Nature* **431**, 549–552 (2004).
- Sleep, N. H. & Hessler, A. M. Weathering of quartz as an Archean climatic indicator. *Earth Planet. Sci. Lett.* **241**, 594–602 (2006).
- Jaffres, J. B. D., Shields, G. A. & Wallmann, K. The oxygen isotope evolution of seawater: a critical review of a long-standing controversy and an improved geological water cycle model for the past 3.4 billion years. *Earth Sci. Rev.* **83**, 83–122 (2007).
- Kasting, J. F. et al. Paleoclimates, ocean depth, and the oxygen isotopic composition of seawater. *Earth Planet. Sci. Lett.* **252**, 82–93 (2006).
- Rye, R. & Holland, H. D. Paleosols and the evolution of atmospheric oxygen: a critical review. *Am. J. Sci.* **298**, 621–672 (1998).
- Ohmoto, H., Watanabe, Y. & Kumazawa, K. Evidence from massive siderite beds for a CO₂-rich atmosphere before 1.8 billion years ago. *Nature* **429**, 395–399 (2004).
- Hoehler, T. M. et al. Comparative ecology of H₂ cycling in sedimentary and phototrophic ecosystems. *Antonie Van Leeuwenhoek Int. J. Gen. Molec. Microbiol.* **81**, 575–585 (2002).
- Kral, T. A., Brink, K. M., Miller, S. L. & McKay, C. P. Hydrogen consumptions by methanogens on the early Earth. *Origins Life Evol. B* **28**, 311–319 (1998).
- Chapelle, F. H. et al. A hydrogen-based subsurface microbial community dominated by methanogens. *Nature* **415**, 312–315 (2002).
- Kasting, J. F., Pavlov, A. A. & Siefert, J. L. A coupled ecosystem-climate model for predicting the methane concentration in the archaic atmosphere. *Origins Life Evol. B* **31**, 271–285 (2001).
- Charecha, P., Kasting, J. & Seifert, J. A coupled atmosphere-ecosystem model of the early Archean Earth. *Geobiology* **3**, 53–76 (2005).
- Rosing, M. T. & Frei, R. U-rich Archean sea-floor sediments from Greenland—indications of > 3700 Ma oxygenic photosynthesis. *Earth Planet. Sci. Lett.* **217**, 237–244 (2004).
- Caballero, R. & Steder, M. *CliMT: An object-oriented Climate Modelling and diagnostics Toolkit*. (<http://maths.ucd.ie/~rca/climt/>) (2008).

Acknowledgements This study was carried out at the Nordic Center for Earth Evolution funded by the Danish National Research Foundation and the research was supported by an Allan C. Cox Professorship to M.T.R. and endowment funds from the Department of Geological and Environmental Sciences from Stanford University to D.K.B., and NSF grants to N.H.S. We are grateful for comments from D. Lowe, D. Canfield, F. Selsis, P. Ditlevsen and the “Ice and climate group” of the Niels Bohr Institute. We thank R. Caballero and J. Bendtsen for comments on the radiation balance model. We thank J. Kasting, A. Lenardic and N. Sheldon for constructive reviews.

Author Contributions All authors have contributed to developing the ideas presented. M.T.R. and D.K.B. carried out the thermodynamic modelling, and C.J.B. carried out the radiative climate modelling, based on surface albedo change (M.T.R.) and low CCN (C.J.B.).

Author Information Reprints and permissions information is available at www.nature.com/reprints. The authors declare no competing financial interests. Correspondence and requests for materials should be addressed to M.T.R. (minik@snm.ku.dk).

METHODS

Thermodynamic modelling of phase equilibria. The partial pressures of CO₂ and H₂ have been calculated assuming they were in equilibrium with minerals and aqueous solutions through reactions (1) to (3), which are relevant for describing the Earth's early surface environments. The equilibrium constants $K_{p,T}$ (where P is pressure and T is temperature) for the limiting reactions (1) to (3) have been calculated at specified pressures and temperatures. We assume that the total atmospheric pressure was 0.1 MPa and that the temperature was either 15 °C, 25 °C or 35 °C as shown in Fig. 1a. The calculations were carried out using the Supcrt computer programme³⁴, using the internally consistent thermodynamic database SLOP98 (http://geopig.asu.edu/supcrt92_data/slop98.dat). Fig. 1a is computed using the gas standard states for H₂ and CO₂, where the aqueous species standard state is adopted for these species in diagram Fig. 1b³⁴.

Climate modelling. In an effort to model the sensitivity of the Earth's surface temperatures under a faint early Sun and with modest CO₂ and CH₄ mixing ratios we have employed a simple standard radiative-convective adjusted radiative equilibrium model³³. The model takes into account the effect of different cloud characteristics during the Archaean owing to lower emissions of CCN from the biosphere and lower surface albedo linked to the gradual growth of continents through geologic time. We constrain the atmospheric CO₂ mixing ratios to be within the limits dictated by the ubiquitous presence of magnetite in Archaean banded iron formations, and allow an atmospheric CH₄: CO₂ ≤ 1, which is arbitrary but within the bounds suggested by refs 8 and 35, and is supported by the observed depletion in H₂ in the Archaean ocean supposedly caused by phototrophic methanogens³².

On the present Earth the hemispherical planetary albedo values are very similar despite the fact that the northern hemisphere has a larger proportion of land surface area compared to the southern hemisphere. By integrating present-day top-of-the-atmosphere albedo along a pure oceanic mid-Pacific longitudinal profile we obtain values of ~0.3 for an Archaean Earth with no continents. This value is not much different from the present global mean top-of-the-atmosphere albedo. However, the probable low productivity of the Archaean^{2,36} would have resulted in a droplet size much bigger than today¹⁴. As a result the atmosphere would be much more transparent to short-wave radiation, for the same water content. The resulting radiation balance would be more sensitive to surface albedo changes, further increasing surface temperatures. As pointed out by ref. 14, the effect of low productivity on droplet size and thus short-wave albedo can be seen over the subtropical gyres, in particular in the south Pacific, where the all-sky top-of-the-atmosphere albedo is about 0.2 locally down to 0.15, as low as the clear-sky albedo. We evaluate the combined effect of changes in mean surface albedo and droplet size with a convective adjusted radiative equilibrium model.

Single-column radiative-convective model. We use a simple standard model of convective adjusted radiative equilibrium based on the CliMT modelling toolkit developed by ref. 33. The model uses the NCAR CCM3 radiation code. A global mean lapse rate of 6.5 K km⁻¹ and present-day CO₂ and CH₄ mixing ratios of 375 and 1.7 p.p.m., respectively, is used³⁷. From General Circulation Model (GCM) calculations³⁸ we find the mean distribution of relative humidity (79, 60, and 50, respectively, for 1000–900 mbar, 900–700 mbar and 700–100 mbar model intervals). Satellite data constrain the global radiation budget, with incident short-wave flux of ~340 W m⁻² and mean outgoing long-wave radiation of 235–240 W m⁻² (that is, planetary albedo of ~0.31) (CERES EBAF Edition1A^{39,40}). The global mean surface albedo is conservatively set to 0.135, approximating a value of 0.144 extracted from model reanalysis data for 2003 (CERES SRBAVG Edition 2⁴⁰). Following others⁴¹ the effective layer cloud water content is adjusted to approximate the radiative effect on short- and long-wave radiative fluxes, respectively, about -47 W m⁻² and ~29 W m⁻² (CERES EBAF Edition1A³⁹). For the clouds we assume a present-day droplet size of 12 μm (ref. 14). Low model clouds are set to fractional cloud cover of 0.5 and cloud water content of 11 g m⁻². High model clouds are set to fractional cloud cover of 0.2 and cloud water content of 3 g m⁻². This results in cloud short- and long-wave radiative effects of -45.8 W m⁻² and 27.8 W m⁻², respectively. These values approximate observations (CERES EBAF Edition1A^{39,40}). With these parameters the calculated mean model surface temperature is 14.3 °C and the planetary albedo is 0.33.

Kump and Pollard¹⁴ estimate that droplet size would possibly increase to 17 μm during the low primary production of the Cretaceous period with fewer CCN. We use the relative humidity distribution from the GCM results³⁸ based on 4 times the PAL p_{CO_2} (relative humidity of 80, 65 and 51 at 1,000–900 mbar, 900–700 mbar and 700–100 mbar intervals, respectively). Then a droplet size of 17 μm and reduced cloud water content has the same radiative warming effect as in the GCM experiments³⁸, which included precipitation enhancement and resulting cloud cover reduction (not modelled explicitly here). Increasing droplet size from 12 μm to 17 μm and decreasing cloud water content to 3.0 g m⁻² decreases

the planetary albedo to 0.23, as shown in Fig. 2c, and increases the model global mean temperature by 10 °C, conservatively similar to the 12 °C of ref. 14.

Estimated surface albedo through time. It is useful to look at how the present albedo can be approximated in simple terms, before calculating the conjectured first-order variation of surface albedo through the Earth's history. The present-day global mean top-of-the-atmosphere albedo ($\alpha_{\text{planetary}} = 0.32$) retrieved from satellite data can simply be approximated by the area-fraction-weighted planetary albedo over land ($\alpha_{\text{planetary land}}$) and ocean ($\alpha_{\text{planetary ocean}}$), that is, $\eta_{\text{land}}\alpha_{\text{planetary land}} + \eta_{\text{ocean}}\alpha_{\text{planetary ocean}}$ where $\eta_{\text{land}} = 0.3$ is the present area fraction of the atmosphere underlain by land, and the ocean fraction is $\eta_{\text{ocean}} = 1 - \eta_{\text{land}}$. Mean top-of-the-atmosphere albedo of longitudinal transects over land gives $\alpha_{\text{planetary land}} \approx 0.35$ (Africa–Europe 24° E) and over ocean $\alpha_{\text{planetary ocean}} \approx 0.3$ (Pacific Ocean, 145° W) (CERES EBAF Edition1A³⁹). This gives $\alpha_{\text{planetary}} \approx 0.315$. Similarly the global mean surface albedo (α_{surface}) can be approximated as the sum of the land fraction albedo ($\eta_{\text{land}} \times 0.23$) and the ocean fraction albedo ($\eta_{\text{ocean}} \times 0.1$), equivalent to the present-day global mean surface albedo of 0.14 as calculated from local short-wave fluxes under all-sky conditions (model reanalysis data for 2003, CERES SRBAVG Edition 2³⁹). The mean surface albedo can also be calculated from the albedo and fractional albedo contributions of different surfaces. The sea surface with light wind waves has a global mean albedo of about $\alpha_{\text{surface ocean}} \approx 0.06$, vegetation-covered continents have an albedo of about $\alpha_{\text{surface land}} \approx 0.21$, snow- and ice-covered regions have an albedo of $\alpha_{\text{surface ice}} \approx 0.5$ (CERES SRBAVG Edition 2^{37,39,42}). Snow and ice cover 7% of the oceans ($\eta_{\text{ocean ice}}$) and 11% of land surface ($\eta_{\text{land ice}}$)³⁷. The resulting mean surface albedo of the Earth is again found to be about $\alpha_{\text{surface}} \approx 0.135$:

$$\alpha_{\text{surface}} = \alpha_{\text{surface ocean}}[\eta_{\text{ocean}}(1 - \eta_{\text{ocean ice}})] + \alpha_{\text{surface land}}[\eta_{\text{land}}(1 - \eta_{\text{land ice}})] + \alpha_{\text{surface ice}}(\eta_{\text{ocean}}\eta_{\text{ocean ice}} + \eta_{\text{land}}\eta_{\text{land ice}}) \quad (5)$$

We use equation (5) to calculate the surface albedo through time with appropriate area fractions and surface albedos as follows: η_{land} is from Fig. 2a, $\eta_{\text{ocean}} = 1 - \eta_{\text{land}}$, and with $\eta_{\text{ocean ice}}$, $\eta_{\text{land ice}}$, α_{ice} and α_{ocean} as today. On the early Earth the land surface albedo (α_{land}) would have been different from today. The first rocks and sediments would have been dominated by black basalts and dark basaltic dust. Black basalt probably has an albedo similar to asphalt pavement (0.07, ranging from 0.05–0.1 (ref. 37)). Moist dark soil typically has an albedo of 0.1 (0.05–0.15). Once granitic rocks and quartz-rich sediment became prevalent the albedo would have increased to 0.3, a value typical of dry desert soil and wet sand (0.20–0.4). Not until the appearance of lichens and vegetation around 1,000 to 450 million years ago would the land surface albedo decrease to present values. To simplify matters, we conservatively assumed that the land surface albedo was 0.3 in the Precambrian period. Snow- and ice-covered regions were present on about 9% of the Earth's surface, as today. In one endmember of our uncertainty calculations we assume that η_{ice} on land and ocean are proportional to the land fraction. From equation (5) we then calculate that a conjectured first-order variation of the surface albedo through the Earth's history would increase from ~0.08, gradually rising to 0.15 in conjunction with continental crustal growth (Fig. 2b). The surface albedo would then decrease to ~0.13 once a terrestrial biosphere was established. The influence of the surface albedo on the planetary albedo is strongly enhanced in an atmosphere with fewer CCN and thus a higher short-wave transparency. In our model we have tested the effect of increased mean droplet sizes from the present-day value of 12 μm up to 17 μm and 30 μm. The effects of increasing the droplet size on the radiative equilibrium temperature are shown in Fig. 2d.

Continental growth. The albedo model above is based on the assumption that the Earth's continents have grown over geologic time. The continents on the Earth are the products of fractionation of the silicate fraction of the planet, nominally the Earth's mantle. The mantle is dominated by Mg–Fe silicate minerals with minor Ca–Al silicate, oxide and sulphide minerals. Most other elements are dissolved as trace components in these major phases. Mantle rocks are dense (~3.4 g cm⁻³) and dark in colour. The continental crust is dominated by granitic rocks which are composed of quartz and feldspar (Ca, Na, K, Al–silicate) with only minor Mg–Fe-bearing minerals such as mica and amphibole. This renders granites light in colour and low in density (~2.5 g cm⁻³). The granitic rocks of the continents cannot be formed by direct partial melting of mantle rocks, because their high silica content is incompatible with the minerals of the mantle. Partial melting of the mantle produces magmas of the basalt family of rocks, which are dark in colour and intermediate in density (~3 g cm⁻³). Basalt is the overwhelmingly dominant component of the oceanic crust, but forms only a minor fraction of the continents. Partial melting of basalt that has previously reacted with water to form hydrous minerals can lead to the formation of granites. The differentiation of

the silicate Earth to form the continents is thus a multi-stage process that relies on the plate tectonic cycling of components between the Earth's reservoirs. The continents, as we understand them today, could not have formed as a protocrust, but must have segregated during a prolonged period of time to allow for all the steps in the multi-stage fractionation process to take place. The time required to build the present continental mass is a matter of considerable controversy. Continental growth models vary between almost-instantaneous formation of the present continental mass, in which recycling of crust to the mantle would balance the formation of new continental crust^{43–45}, and other models based on the trace-element fractionation history of the Earth's mantle, which suggest that the continental crust grew over geologic time, with varying rates of growth and possibly episodically^{46–49}.

In a geologic sense, emergent land is not necessarily continental, and all continental areas are not necessarily emergent, as exemplified by the continental shelf, which is continental in composition but submerged under the sea, versus Hawaii and Iceland, which are emergent but are composed of oceanic crust. The relationship between the mass fraction of the silicate Earth that is compartmentalized into the continents and the surface fraction of the Earth covered by emergent continents is also a matter of poor understanding and ongoing controversy^{50,51}. From the perspective of the Earth's albedo, the important parameter is the surface fraction of emergent continental rocks, and in our models we have made the assumption that emergent continental surface area scales with the mass of the continents. Note that in Fig. 2a, we have adopted various scenarios for the growth of continental mass as a function of geologic time, such that the full range between the proposed endmember models is tested in our model for the early Earth's climate.

34. Johnson, J. W., Oelkers, E. H. & Helgeson, H. C. Supcrt92—a software package for calculating the standard molal thermodynamic properties of minerals, gases, aqueous species, and reactions from 1-bar to 5000-bar and 0-degrees-C to 1000-degrees-C. *Comput. Geosci.* **18**, 899–947 (1992).
35. Pavlov, A. A., Kasting, J. F., Brown, L. L., Rages, K. A. & Freedman, R. Greenhouse warming by CH₄ in the atmosphere of early Earth. *J. Geophys. Res.* **105**, 11981–11990 (2000).
36. Bjerrum, C. J. & Canfield, D. E. Ocean productivity before about 1.9 Gyr ago limited by phosphorus adsorption onto iron oxides. *Nature* **417**, 159–162 (2002).
37. Hartmann, D. L. *Global Physical Climatology* (Academic Press, 1994).
38. Kump, L. R., Kasting, J. F. & Barley, M. E. Rise of atmospheric oxygen and the “upside-down” Archean mantle. *Geochem. Geophys. Geosyst.* **2**, 2000GC000114 (2001).
39. Wielicki, B. A. *et al.* Clouds and the Earth's radiant energy system (CERES): an Earth observing system experiment. *Bull. Am. Meteorol. Soc.* **77**, 853–868 (1996).
40. Kiehl, J. T. & Trenberth, K. E. Earth's annual global mean energy budget. *Bull. Am. Meteorol. Soc.* **78**, 197–208 (1997).
41. Caldeira, K. & Kasting, J. F. The life-span of the biosphere revisited. *Nature* **360**, 721–723 (1992).
42. Peixoto, J. P. & Oort, A. H. *Physics of Climate* (American Institute of Physics, 1992).
43. Armstrong, R. L. The persistent myth of crustal growth. *Aust. J. Earth Sci.* **38**, 613–630 (1991).
44. Wilde, S. A., Valley, J. W., Peck, W. H. & Graham, C. M. Evidence from detrital zircons for the existence of continental crust and oceans on the Earth 4.4 Gyr ago. *Nature* **409**, 175–178 (2001).
45. Valley, J. W. *et al.* A cool early Earth. *Geology* **30**, 351–254 (2002).
46. McLennan, S. M. & Taylor, S. R. Continental freeboard, sedimentation rates and growth of continental crust. *Nature* **306**, 169–172 (1983).
47. Collerson, K. D. & Kamber, B. S. Evolution of the continents and the atmosphere inferred from Th-U-Nb systematics of the depleted mantle. *Science* **283**, 1519–1522 (1999).
48. Nagler, T. F. & Kramers, J. D. Nd isotopic evolution of the upper mantle during the Precambrian: models, data and the uncertainty of both. *Precamb. Res.* **91**, 233–252 (1998).
49. Condie, K. C. Episodic continental growth models: afterthoughts and extensions. *Tectonophysics* **322**, 153–162 (2000).
50. Flament, N., Coltice, N. & Rey, P. F. A case for late-Archaean continental emergence from thermal evolution models and hypsometry. *Earth Planet. Sci. Lett.* **275**, 326–336 (2008).
51. Rey, P. F. & Coltice, N. Neoproterozoic lithospheric strengthening and the coupling of Earth's geochemical reservoirs. *Geology* **36**, 635–638 (2008).